Available online at www.sciencedirect.com
ScienceDirect
Trans. Nonferrous Met. Soc. China 20(2010) 624−631
Transactions of Nonferrous Metals Society of China
www.tnmsc.cn

Fabrication of ultrahigh density ZnO-Al_2O_3 ceramic composites by slip casting

SUN Yi-hua(孙宜华)[1, 2], XIONG Wei-hao(熊惟皓)[2], LI Chen-hui(李晨辉)[2]

1. College of Mechanical and Material Engineering, China Three Gorges University, Yichang 443002, China;
2. State Key Laboratory of Material Processing and Die & Mould Technology, Huazhong University of Science and Technology, Wuhan 430074, China

Received 23 February 2009; accepted 22 September 2009

Abstract: The conditions of ZnO-Al_2O_3 aqueous suspensions and slip casting were optimized to obtain dense green compacts and further to obtain high density ZnO-Al_2O_3 ceramic composites. The Zeta potential of raw powders was measured. ZnO and Al_2O_3 powders have lower Zeta potential than −45 mV commonly at pH 8−10.3 with polyacrylic acid (PAA) added. The influence of pH and the mass fraction of the additives on the stability and fluidity of the suspensions added with PAA and polyethylene glycol (PEG) was investigated by experiments of viscosity and sedimentation. The suspensions have the lowest viscosity and the best stability at pH 9 with 0.2% PAA (mass fraction). The maximum density of green compacts is 66.6% of theoretical density (TD) with compacting and homogeneous green particles. An ultrahigh density sintered compact (＞99.6% TD) could be obtained after pressureless sintering at 1 400 ℃ for 2 h.

Key words: ZnO-Al_2O_3 mixture; suspension; slip casting; sintering; ceramics

1 Introduction

Aluminium-doped zinc oxide (AZO) thin films that have more potential than indium-tin oxide (ITO) films are increasingly used as the transparent and conductive electrodes for several optoelectronic devices such as photovoltaic solar cells, liquid crystal displays or light emitting diodes[l−4]. Nowadays, many techniques for the deposition of AZO thin films have been developed but the most widely used commercial method is magnetron sputtering, which is mainly owing to some of its merits such as high deposition speed and good adhesion. The metallic, alloyed, or ceramic targets have been used for production by different modes including continuous or pulsed direct current (DC) as well as radio-frequency (RF) sputtering[5−9]. The metallic or alloyed targets reacting in reactive atmosphere makes the processes difficult to control and guarantee stable oxide film formation at high deposition rates[7−8]. Therefore, the sputtering of ceramic targets is one of the preferable choices to be used for continuous or pulsed DC plasma excitation, thus avoiding the need for reactive process control equipment and also the complexity of RF matching circuits[9].

The high density of ceramic targets of sputtering plays an important role in the sputtering process and the final quality of thin films[10], but in terms of the authors' knowledge, the most of ceramic targets of sputtering have relative density less than 97.5% of theoretical density (TD). The manufacturing of large-sized fully dense ceramic targets is quite challenging for commercial ceramic processing[10]. Slip casting is a well-known forming method for ceramics, which is a suitable consolidation process to obtain materials with high green density and microstructure homogeneity[11]. The goal of dispersion in this process is to achieve a high solid loading suspension with a high degree of stability. Very high green densities are easily obtained with well dispersed slips but the slip-casting green compacts are very brittle, therefore, binders added are necessary. The high green density and the microstructure homogeneity are advantageous to reach the highest sintered density[12]. The aim of this work is to optimize the conditions of the well-dispersed suspensions in order to produce dense and homogeneous green compacts of ZnO-Al_2O_3 mixtures by a slip casting process, and then to obtain ultrahigh density ZnO-Al_2O_3 ceramic composite targets after pressureless sintering. This technological line is a low cost and environment-friendly process.

Foundation item: Project(50477044) supported by the National Natural Science Foundation of China
Corresponding author: LI Chen-hui; Tel: +86-27-63049732; E-mail: li_chenhui@sohu.com
DOI: 10.1016/S1003-6326(09)60189-8

2 Experimental

Commercial zinc oxide and alumina powders (Sumitomo, Japan, 99.99% purity), which had specific surface areas (BET) of 10.8 m^2/g and 8.9 m^2/g respectively and average particle sizes around 260 nm and 320 nm respectively, were used. A polyacrylic acid (PAA, MW5000) and a polyethylene glycol (PEG, MW40000) were used as a deflocculant agent and a binder agent respectively.

Zeta potential was measured on a Zeta-potential analyzer (90Plus, Brookhaven Instruments Co., USA) to determine the surface charge of the particles at a constant temperature of 25 ℃. Slurries mixed with de-ionized water, additives, and mixtures of ZnO and Al_2O_3 powders (the mass ratio is 98:2) were prepared at solids content 70% (mass fraction, the same below if not mentioned) (corresponding to 30% of volume fraction, on the basis of dry powder mass). The pH was adjusted with ammonia (25%). The slurries were treated by ball-milling with zirconia grinding media for 36 h and subsequently degasing under vacuum. Apparent viscosity of the prepared slurries was measured using a digital rotational viscometer (Brookfield RVDV-E, Brookfield Engineering Laboratories, Inc.) at the shear rates of 9.3, 18.6, 46.5, and 93 s^{-1} at 25 ℃. Slurry stability was evaluated in each sample of as-prepared slurry, by measuring the particles settling rate inside glass test tubes of 100 mL for 5 d. The as-prepared slurries were taken out 10 mL suspension and the slurries settled for 36 h were taken out 10 mL suspension respectively from their top, middle and bottom by a needle tube, and then these specimens were dried and powdered. The dispersion of alumina was examined by X-ray diffraction analysis (XRD, X'Pert PRO, PANalytical B.V. Co. Ltd.) with a Cu K_α radiation (λ=1.540 6 Å) operated at 40 kV and 40 mA.

The as-prepared slurries were poured into white plaster molds for the production of two kinds of specimens: cylindrical rods (d 16 mm×16 mm) for the measurements of radial crushing strength and cubical bar (12 mm×9 mm×45 mm) for sintering. After casting, the specimens were sintered at 110 ℃ for 2 h and then fired at 1 400 ℃ for 2 h with a heating rate of 5 ℃/min. The densities of green and sintered bodies were evaluated by the Archimedes method using mercury displacement. The radial crushing strength of the green compacts was investigated by performing crushing tests in a mechanical testing device (Instron3369, Instron Corp., USA), of which the values obtained are arithmetic mean value of six measured specimens. The polished sintered samples were thermal-etched at 1 150 ℃ for 10 min. The fracture and thermal-etched surface of the samples were analyzed using a scanning electron microscope (SEM, FEI Quanta 200 microscope, Holland FEI Co.) equipped with an energy-dispersive spectrometer (EDS).

3 Results and discussion

3.1 Zeta potential measurement

Zeta potentials of ZnO and Al_2O_3 powders were measured respectively without and with the addition of polyacrylic acid (PAA) only or PAA+PEG (polyethylene glycol). As shown in Fig.1, the Zeta potential of ZnO without additives is low, which means that ZnO powders could not be stable in aqueous solution only depending on adjusting pH values without any additives. When the dispersant of PAA is added to suspensions, isoelectric point (IEP) of both ZnO and Al_2O_3 are dramatically shifted towards acidic values from pH 9.2 to 5.0 and from pH 8 to 3.9 respectively, while the Zeta potentials (absolute value) of both ZnO and Al_2O_3 are augmented in the alkaline range. On the other hand, when adding PEG simultaneously, in contrast with only adding PAA, the IEP of ZnO and Al_2O_3 are not shifted and their Zeta potentials are scarcely influenced. Since the carboxyl groups can dissociate from PAA in aqueous solution which bond with the particles mainly depending on chemical interaction, the observed lowering of Zeta potential results from the lowering of the surface charge and the increase of negatively charged —COO^- groups distributed along the polymer chains. This change may be also attributed to the blockage of active sites on the particle surface and the influence of the slippage plane of the electrical double layer away from the surface by adsorption of polymer chain[13]. Whereas, the charge of the particle surface is hardly affected by PEG because of PEG bonding with particles surface mainly through hydrogen bonding[14]. Nevertheless it is important that these two kinds of powders have higher Zeta potential of absolute value (＞45 mV) in common basic range from

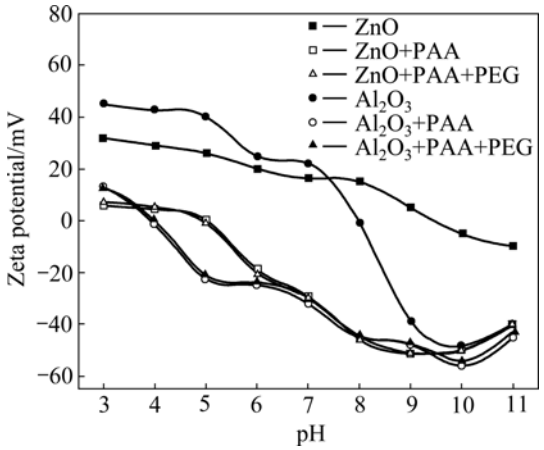

Fig.1 Zeta potential of zinc oxide and alumina as function of pH in absence and presence of PAA and PEG

pH 8 to 10.3 when adding PAA, which makes it possible that the mixed powders could be stabilized together in the aqueous suspensions.

3.2 Dispersion of slurries

Fig.2 shows the apparent viscosity and the sediment height as functions of the additive amount of PAA for the slurries with 0.2% PEG at pH 9. The apparent viscosity was numerated at the shear rate of 93 s^{-1}. The lowest viscosity and the highest sediment are obtained at 0.2% PAA, indicating that the 0.2% PAA could equal to the saturated adsorption amount. For w(PAA)＜0.2% the increase in the viscosity and the decrease in the sediment height are due to incomplete adsorption, which results in lower electrostatic repulsion between particles, thereby forcing particles together. On the other hand, for w(PAA)＞0.2%, a probably excess of PAA in solution could not only increase the ionic strength of the solution to compress the double layer, which results in the electrostatic repulsion reducing between particles[15], but also increase the bridging flocculation, which results from polyelectrolyte macromolecule. In the latter two cases above, the slip viscosity increases and the stability of slurries decreases.

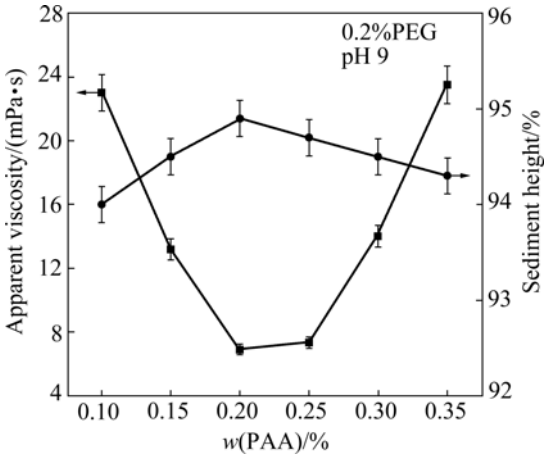

Fig.2 PAA content as functions of viscosity and sediment height of slurries

Fig.3 shows the relationship between the apparent viscosity and the shear rate when different amounts of PEG additions were used with 0.2% PAA at pH 9. The apparent viscosity increases with the amount of PEG increasing. At low PEG levels, the ZnO-Al_2O_3 slurries show a Newtonian behavior. And then, up to 0.2% PAA, the slurries show near-Newtonian behavior, while the viscosity increases a little. With the amount of PEG further increasing, the viscosity increases dramatically and the slurries turn to be non-Newtonian behavior. The flow curves deviate Newtonian fluid, and that the apparent viscosity descends while shear rate ascends, which is the shear-thinning phenomenon in rheology. The shear thinning behavior that is clearly observed at high PEG level might due to the breakdown of the entanglement of the polymer chains[16], and the flocculation distinctly occurred in ZnO-Al_2O_3 slurries. Since the concentration of remainder PEG in the solution increased when the amount of PEG increasing, the slurry viscosity also increased. The remainder PEG in the solution promoted flocculation through bridge action. Especially when w(PEG)＞0.2%, the apparent viscosity and the flocculation increased remarkably. So this condition in 0.2% PEG could be selected for further work.

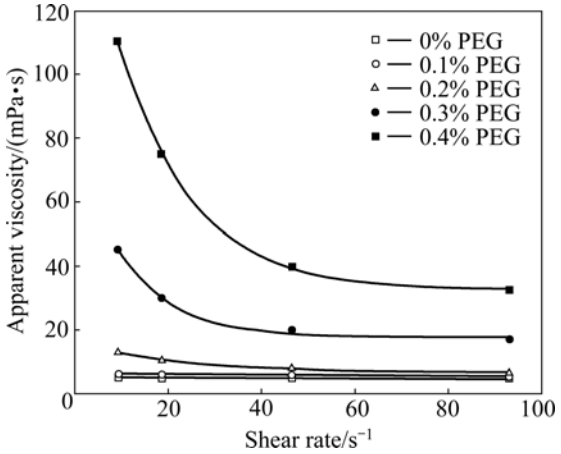

Fig.3 Flow curves of viscosity vs shear rate as function of PEG content

Fig.4 shows the apparent viscosity and the sediment height as functions of pH for the slurries with 0.2% PAA and 0.2% PEG. The apparent viscosity was numerated at the shear rate of 93 s^{-1}. In the region of pH 8−10.3, the slurries are more stable and their viscosities are lower than remainder regions of pH. At pH 9, the slurry viscosity is the lowest (6.9 mPa·s) and the sediment height is the highest (95.3%). Since the change of pH can influence not only the potential of particles surface but also the ionization degree and adsorption configuration of polymer[17]. The degree of ionization of PAA increases from 0 to 1 when pH changes from 3 to 9[18]. The increasing pH results in the increase of the negative charge of solid surface and PAA adsorbed on it almost totally ionized at pH 8−10.3, which causes enlarging Zeta potential and enhancing electrostatic repulsion. At the same time, the loops and tails configurations of polymer are so dominant that the steric repulsion is also much stronger. However, the adsorption amount of PAA decreases with pH increasing and then the remains of PAA in solution would augment the slurry viscosity [19]. Besides, with pH further increasing, the ion concentration in solution increases which results in the double layer to be compressed and the Zeta potential being reduced[15]. So the electrosteric repulsion between

particles is reduced, which results in increasing the slip viscosity and decreasing the slurry stability. Consequently, the optimum dispersing condition is reached for the slurries by the electrosteric repulsion at pH 9. These results are consistent with the Zeta potential analysis.

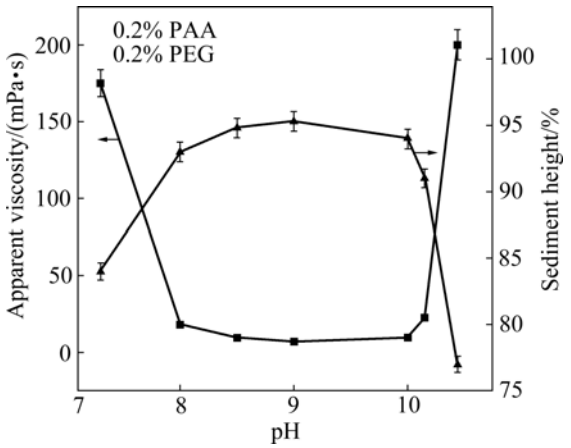

Fig.4 Relationships between pH and apparent viscosity or sediment height of slurries

In order to verify the dispersion of alumina, the mixed ZnO-Al_2O_3 powders were measured by X-ray diffraction analysis. Fig.5 shows the XRD patterns of mixed ZnO-Al_2O_3 powders derived from the as-prepared slurry and the top, middle, and bottom of the slurries settled for 36 h respectively with 0.2% PAA and 0.2% PEG at pH 9. As shown on the left of Fig.5, the main peaks are almost the same in position and relative intensity as those of the ZnO raw powder. The figures on the right of Fig.5 show magnified profiles around the α-Al_2O_3 (113) peak, which has the highest intensity in

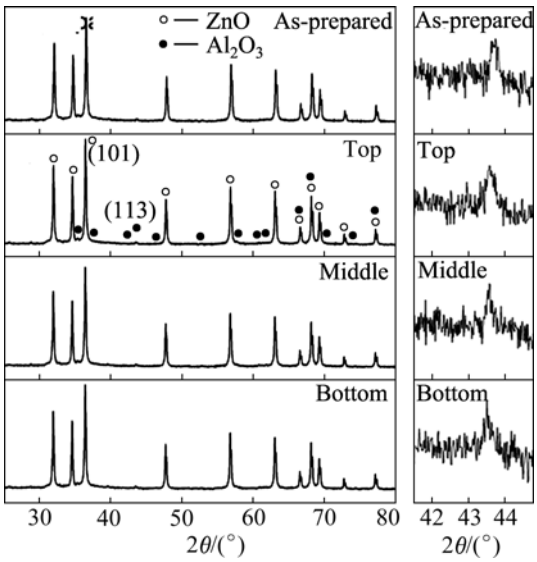

Fig.5 XRD patterns of mixed ZnO-Al_2O_3 powders (Magnified patterns around α-Al_2O_3 (113) peak are shown on the right)

α-Al_2O_3 powder diffraction. It is obvious that the position and relative intensity of the α-Al_2O_3 (113) peaks are scarcely changed in the all specimens, The peak intensity ratios of Al_2O_3 (113) to ZnO (101) + Al_2O_3 (113) of the top, middle, and bottom layers are 3.3962×10^{-3}, 3.0423×10^{-3}, 3.6065×10^{-3} respectively. It is clearly seen that the α-Al_2O_3 particles could be equably distributed in each layer of the slurry during process time.

3.3 Green and sintered compacts

In our previous study, the theoretical densities of the green and sintered compacts of the 98% ZnO-2% Al_2O_3 ceramics are 5.671 g/cm^3 and 5.673 g/cm^3 respectively [20]. Fig.6(a) shows the green compact density and strength versus the amount of PAA added at pH 9 with 0.2% PEG. The better slip dispersion has achieved for about 0.2% PAA and results in the highest green density value. At PAA contents of 0.2% the adsorbed amount is sufficient to enhance the electrosteric repulsion between particles that assisted to obtain a more efficient packing of the particles. In general, small dispersant concentrations are not adequate to fully deflocculate the slurry and maintain the colloidal particles in suspensions. On the other hand, the high dispersant concentrations result in an increase in viscosity as well. For PAA additions lower than 0.2%, a remarkable decrease in the green compact density can be found in accordance with the increase in the slip viscosity (Fig.4 and Fig.6(a)) owing to incomplete adsorption of PAA. GARRIDO et al[12] explained that an incomplete coverage of particles surface at low dispersant levels reduce the net negative surface charge of the mixtures. Therefore, this result is due to low electrostatic repulsion between particles. On the contrary, the decrease in the green compact density for PAA additions higher than 0.2% is consistent with the increase in the slip viscosity (Fig.4 and Fig.6(a)) owing to excess of PAA. However, the density of green compacts prepared from suspensions containing excess of PAA show a relatively slower decrease than that produced from suspensions containing an insufficient amount of PAA. Since large amounts of free PAA in solution enhancing an additional steric contribution due to higher adsorbed amounts and a change in configuration of the adsorbed molecule. The additional steric repulsion may prevent close contact between particles as the interparticle distance decreased during consolidation[12]. In this weakly flocculated suspensions the presence of short-range repulsive potentials between particles may reduce interfacial friction, facilitating particle sliding and arrangement. Nevertheless, to sum up, a correlation between the green compact density and the viscosity could be found, as the slip viscosity is decreased, a denser packing sample is obtained.

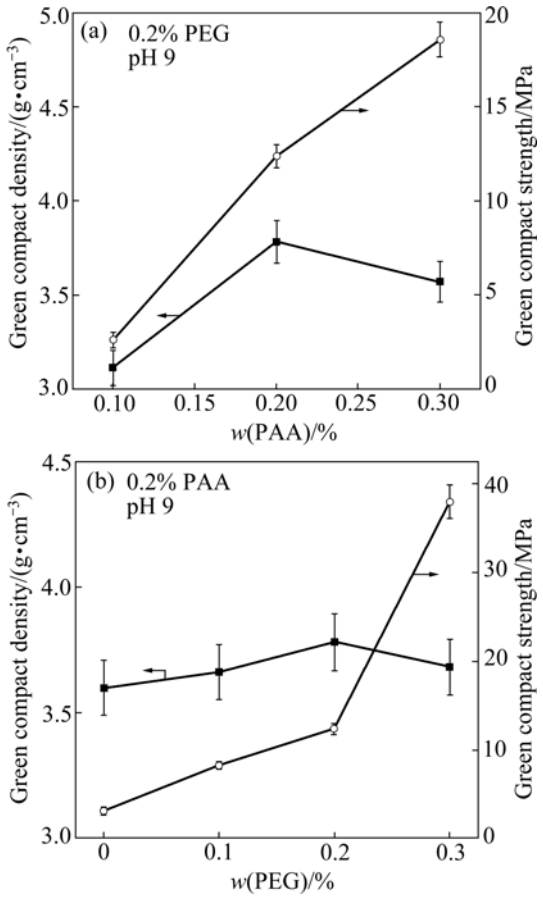

Fig.6 Relationship among green compact density, compact strength and PAA (a) and PEG (b)

Fig.6(b) shows the green compact density and strength versus the amount of PEG added at pH 9 with 0.2% PAA. The highest green density has obtained with about 0.2% PEG. In general, the lower the viscosity is, the higher the green density is. But the viscosity of the suspensions with 0.2% PEG is slightly higher than that with 0.1% PEG. A possible explication is that some PEG absorbed on the particles could produce some steric repulsion and then these repulsive potentials between particles could reduce interfacial friction also, facilitating particle sliding and arrangement. With the amount of PEG further increasing (＞0.2%), the viscosity of the suspensions increases dramatically, the slurries turn to be non-Newtonian fluid, the flocculation distinctly occurs in ZnO-Al_2O_3 slurries, and then the green density deceases as well.

Besides, it is obvious that the green compact strength increases with the amount of added polymers increasing, both for PAA and PEG (Figs.6(a) and 6(b)). However, a poor characteristic of slurries and a decrease of green density occur when only using PAA added to improve the green compact strength, so that PEG added is necessary. When adding with 0.2% PEG, the characteristics of slurries are not influenced remarkably, but the green compact strength is increased to 12.5 MPa. This is advantageous to the conditions of actual operation because the green compact without binders has quite a low strength and is easily broken. For example, adding with 0.2% PAA at pH 9 but without PEG, the green compact strength is only 3.1 MPa or so.

The fracture surface of the green compact with 0.2% PAA and 0.2% PEG at pH 9 is shown in Fig.7. It can be seen that the green particles are packed in a compacting and homogeneous case. The maximum density of green compact is obtained using the ZnO-Al_2O_3 mixture powders, which is close to the value corresponding to an optimum particle packing. The maximum green density value is 66.6% of TD. In our case, the viscosity of ZnO-Al_2O_3 mixture slurries reaches minimum after ball milling for 36 h and that the shear thinning or the shear thickening characteristics become less evident. These results could be attributed to the deagglomerating/ milling effect, leading to a more favorable particle size distribution[21]. The less resistance offered by the suspensions to flow means that the packing ability of the systems has improved[22].

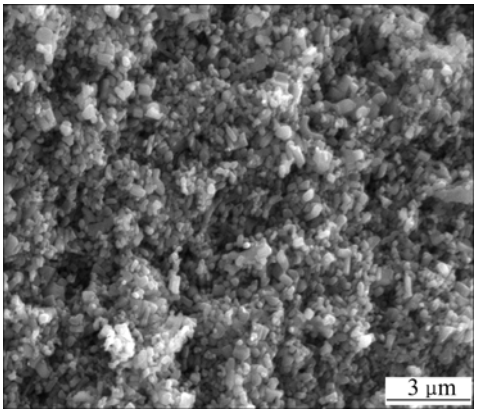

Fig.7 SEM image of fracture surface of green compact with 0.2% PAA and 0.2% PEG at pH 9

The green compacts prepared from the suspensions containing 0.1%−0.5% of PAA and PEG at pH 8, 9, and 10 were selected to sinter at 1 400 ℃ for 2 h. The density of sintered samples is compared with the green density in Fig.8. The correlation coefficient (0.862) indicates that the density after sintering is related to the green density, in other words, the high green density gives the highest sintering density. According to WEI et al[23] the highest sintering density is obtained when the microstructure has the smallest most frequent pore diameter and the smallest pore size distribution. In our case, since the concentration of Al_2O_3 powders is small (2%) in the mixtures and the average size of Al_2O_3 powders is close to ZnO powders, after milling for 36 h, the Al_2O_3 particles distributed in the slurry were homogeneous and stable. Thus, the consolidation

mechanism during slip-casting depends primarily on the slurry viscosity[24]. The different additives or different amount of additives added would influence the rheology of slurries and the consolidation mechanism during slip-casting, and cause different sizes and distributions of pores by agglomeration or flocculation in green compacts. The more the flocculation is, the bigger the average size of pores is and the worse the pore size distribution is. Thereafter, the sintering of ceramic materials depends principally on the pore size distribution and the homogeneity of sample porosity. In the sintering of homogeneity of samples of uniform particles, the uniform interstices that are smaller than the grains retract quite rapidly and evenly[25]. Therefore, the green compacts of high density with small and uniform pores would give the high sintered density.

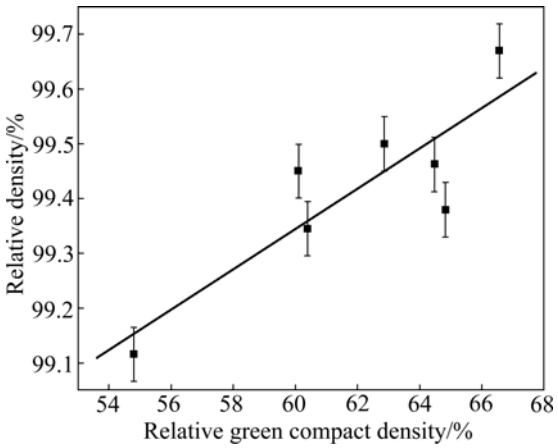

Fig.8 Comparison of density after sintered in relation to green density

Fig.9 shows the SEM micrographs of fracture surfaces of the samples with 0.1% or 0.2% PAA and with 0.2% PEG at pH 9 after sintering at 1 400 ℃ for 2 h. It can be seen from the SEM images, the presence of some closed pores entrapped at the grain boundaries and located at the triple points. These pores are well distributed in the both specimens, but the size of pores is 1.5 μm or less in Fig.9(a) and 1 μm or less in Fig.9(b). The amount of pores in Fig.9(a) seems also more than in Fig.9(b). Since the slurry with 0.1% PAA is slightly flocculated and its green density is only 54.8% of TD, and then its final sintered density is lower (99.1% of TD). Consequently in this specimen the pores are bigger and their amount is more than the other one. The grains cleavage can be seen in the SEM images that the fractures occur through the grains in both sintered specimens.

Fig.10 shows the ESEM micrographs of thermal-etched surfaces of the sintered specimen with 0.2% PAA and 0.2% PEG at pH 9. It can be seen in Figs.10(a) and

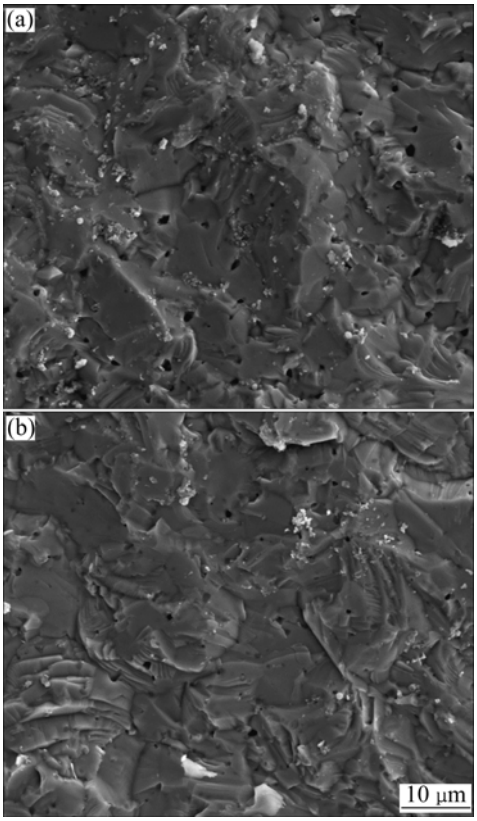

Fig.9 SEM images of fracture surface of sintered samples with 0.2% PEG at pH 9: (a) With 0.1% PAA; (b) With 0.2% PAA

10(b), the microstructure of the sintered specimen is very homogeneous without abnormal grain growth and free of defects. The average grain sizes of the thermally etched specimen are between 4 and 8 μm. The backscattered electron images and energy dispersive X-ray spectrogram of the specimen are also given in Fig.10. It is clear that the off-white regions are ZnO phases and the dark regions are Al-rich phases in Fig.10(c). A homogeneous distributed Al-rich phase is clearly visible as dark patches in sizes of 1−3 μm or so at the ZnO grain boundaries and in the ZnO grains, predominantly located at the triple points. As shown in Fig.10(d), the result of the EDS analysis reveals that the Al content in the Al-rich phase was 5.16% (mole fraction). The homogeneous distribution of Al species in the microstructure of ZnO-Al_2O_3 ceramics is of paramount importance to the final quality of sputtering thin films. It should be noted that a near-to-theoretical compact (＞ 5.66 g/cm^3) can be obtained, which is the samples prepared with 0.2% PAA and 0.2% PEG at pH 9 after sintering at 1 400 °C for 2 h. The relative density is confirmed to be more than 99.6% of TD.

4 Conclusions

1) Zeta potential analysis shows that ZnO and Al_2O_3

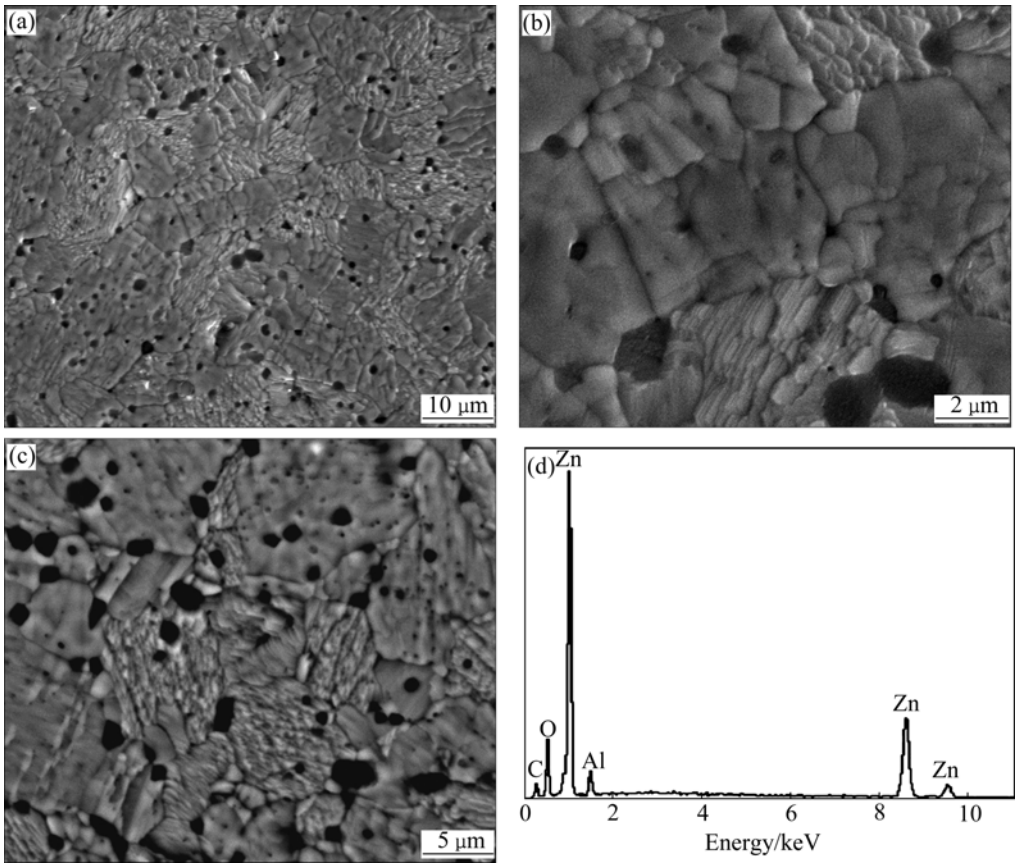

Fig.10 ESEM images of thermal-etched surface of sintered samples with 0.2% PAA and 0.2% PEG at pH 9: (a), (b) In secondary electron mold; (c) In backscattering mold; (d) EDS pattern of dark region

powders have lower Zeta potential than −45 mV commonly at pH 8−10.3 after polyelectrolyte PAA was added, which pave the way for the simultaneous dispersion of ZnO-Al_2O_3 mixtures in aqueous solution.

2) Aqueous suspensions of ZnO-Al_2O_3 mixtures have been prepared at solid loadings of 30% (volume fraction) by dispersing with 0.2% PAA and 0.2 % PEG at pH 9. Under these conditions, the slurry viscosity is the lowest (6.9 mPa·s) and the sediment height is the highest (95.3%). Since 0.2% PAA could equal to the saturated adsorption amount for the ZnO-Al_2O_3 mixtures which results in well-dispersed slurry. On the other hand, it is advantageous to subsequent process as compared with without binder that the green compact strength increased to 12.5 MPa with 0.2% PEG. XRD analysis shows that Al_2O_3 particles are stably distributed in each layer of the slurries.

3) Slip casting of the optimized suspensions leads to the maximum green density greater than 66.6% of TD and the green particles of ZnO-Al_2O_3 mixtures are packed in the compactly homogeneous state. After pressureless sintering at 1 400 ℃ for 2 h, an almost full density compact (＞99.6% of TD) can be obtained. The microstructure observations reveal that very homogeneous materials are obtained without abnormal grain growth and free of defects and with homogeneous distribution of Al species. Slip casting allows the manufacturing of defect-free, homogeneous, and near-to-theoretical density of ZnO-Al_2O_3 ceramics.

References

[1] DAI L P, DENG H, MAO F Y, ZANG J D. The recent advances of research on p-type ZnO thin film [J]. J Mater Sci: Mater Electron, 2008, 19(8/9): 727−734.

[2] RUSKE F, PFLUG A, SITTINGER V, WERNER W, SZYSZKA B, CHRISTIE D J. Reactive deposition of aluminium-doped zinc oxide thin films using high power pulsed magnetron sputtering [J]. Thin Solid Films, 2008, 516(14): 4472−4477.

[3] OH B Y, JEONG M C, MOON T H, LEE W, MYOUNG J M, HWANG J Y, SEO D S. Transparent conductive Al-doped ZnO films for liquid crystal displays [J]. J Appl Phys, 2006, 99(12): 124505−4.

[4] HAO X T, ZHU F R, ONG K S, TAN L W. Hydrogenated aluminium-doped zinc oxide semiconductor thin films for polymeric light-emitting diodes [J]. Semicond Sci Technol, 2006, 21(1): 48−54.

[5] YASUI K, ASANO A, OTSUJI M, KATAGIRL H, MASUDA A, NTSHIYAMA H, INOUE Y, TAKATA M, AKAHANE T. Improvement of the uniformity in electronic properties of AZO films using an RF magnetron sputtering with a mesh grid electrode [J]. Mater Sci Eng B, 2008, 148(1/3): 26−29.

[6] HERRMANN D, OERTEL M, MENNER R, POWALLA M. Analysis of relevant plasma parameters for ZnO: Al film deposition based on data from reactive and non-reactive DC magnetron

sputtering [J]. Surf Coat Technol, 2003, 174/175: 229−234.

[7] RUSKE F, PFLUG A, SITTTINGER V, WERNER W, SZYSZKA B. Process stabilisation for large area reactive MF-sputtering of Al-doped ZnO [J]. Thin Solid Films, 2006, 502(1/2): 44−49.

[8] KELLY P J, ZHOU Y J. Zinc oxide-based transparent conductive oxide films prepared by pulsed magnetron sputtering from powder targets: Process features and film properties [J]. Vac Sci Technol A, 2006, 24(5): 1782−1785.

[9] KLUTH O, SCHOPE G, RECH B, MENNER R, OERTELLL M, ORGASSA K, SCHOCK H W. Comparative material study on RF and DC magnetron sputtered ZnO:Al films [J]. Thin Solid Films, 2006, 502(1/2): 311−316.

[10] LIU C P, JENG G R. Properties of aluminum doped zinc oxide materials and sputtering thin films [J]. J Alloys Compd, 2009, 468(1/2): 343−349

[11] LANGE F F. Powder processing science and technology for increased reliability [J]. J Am Ceram Soc, 1989, 72(1): 3−15.

[12] GARRIDO L B, AGLIETTI E F. Pressure filtration and slip casting of mixed alumina- zircon suspensions [J]. J Eur Ceram Soc, 2001, 21(12): 2259−2266.

[13] LIUFU Sheng-cong, XIAO Han-ning, LI Yu-ping. Adsorption of poly(acrylic acid) onto the surface of titanium dioxide and the colloidal stability of aqueous suspension [J]. J Colloid Interface Sci, 2005, 281(1): 155−163.

[14] LIUFU Sheng-cong, XIAO Han-ning, LI Yu-ping. Investigation of PEG adsorption on the surface of zinc oxide nanoparticles [J]. Powder Techn, 2004, 145(1): 20−24.

[15] CESARANO Ⅲ J, AKSAY I A. Processing of highly concentrated aqueous alumina suspensions stabilized with polyelectrolytes [J]. J Am Ceram Soc, 1988, 71(12): 1062−1067.

[16] OTSUBO Y. Normal stress behavior of highly elastic suspensions [J]. J Colloid Interf Sci, 1994, 163(2): 507−511.

[17] LEWIS J A. Colloidal processing of ceramics [J]. J Am Ceram Soc, 2000, 83(10): 2341−2359.

[18] KIRBY H G, HARRIS D J, LI Q, LEWIS J A. Poly(acrylic acid)-poly(ethylene oxide) comb polymer effect on $BaTiO_3$ nanoparticle suspension stability [J]. J Am Ceram Soc, 2004, 87(2): 181−186.

[19] SANTHIYA D, SUBRAMANIAN S, NATARAJAN K A. Surface chemical studies on the competitive adsorption of poly(acrylic acid) and poly(vinyl alcohol) onto alumina [J]. J Colloid and Interface Sci, 1999, 1216(1): 143−153.

[20] SUN Y H, XIONG W H, LI C H. Effect of Dispersant concentration on preparation of an ultrahigh density ZnO-Al_2O_3 target by slip casting [J]. J Am Ceram Soc, 2009, 92(9): 2168−2171.

[21] KHALIL K A, KIM S W. Mechanical wet-milling and subsequent consolidation of ultra-fine Al_2O_3-(ZrO_2+3%Y_2O_3) bioceramics by using high-frequency induction heat sintering [J]. Trans Nonferrous Met Soc China, 2007, 17(1): 21−26.

[22] OLHERO S M, FERREIRA J M F. Particle segregation phenomena occurring during the slip casting process [J]. Ceram Int, 2002, 28(4): 377−386.

[23] WEI J W C, LU S J, YU B. Characterization of submicron alumina dispersion with poly(methacrylic acid) polyelectrolyte [J]. J Eur Ceram Soc, 1995, 15(2): 155−164.

[24] TSETSEKOU A, AGRAFIOTIS C, MILIAS A. Optimization of the rheological properties of alumina slurries for ceramic processing applications (Part I): Slip-casting [J]. J Eur Ceram Soc, 2001, 21(3): 363−373.

[25] GARCIA DOS SANTOS I M, MOREIRA R C M, LEITE E R, LONGO E, VARELA J A. Sintering of zirconia composites by slip casting [J]. Ceram Int, 2001, 27(3): 283−289.

(Edited by LI Xiang-qun)